Part A: English Edition

Journal of Textiles and Polymers

Vol. 9, No. 1, 3-11, 2021

ORIGINAL PAPER

Parameter Estimation of Viscoelastic Model to Simulate the Compression Behavior of Artificial Grass under Dynamic Loading Using Imperialist Competitive Algorithm

Abas Ali Azami, Pedram Payvandy*, and Mohammad Mahdi Jalili

Received: 9 April 2020, accepted: 7 July 2020

***Abstract*- In this study, the parameters of linear Jeffrey's model are estimated using imperialist competitive algorithm to simulate the compression behavior of artificial grass under dynamic loading. To this end, a viscoelastic model is used to explain this behavior according to ISO 2094. The model consists of a linear spring and a dashpot set parallel to each other. This combination is placed in series with a linear dashpot. The Fourier transform periodic excitation is converted to the summation of harmonic forces. Then, differential equations of the system motion are solved analytically. The result predicted for the compression behavior of artificial grass in dynamic loading is compared with the experimental results. According to the results, the average value of error for prediction of the compression behavior is 5.68%. Therefore, the linear Jeffrey's II model has a high ability to predict the compression behavior of artificial grass under dynamic loading.**

***Keywords*: compression, artificial grass, linear Jeffrey's II model, imperialist competitive algorithm, dynamic loading, fourier transform**

I. INTRODUCTION

Artificial grass has various applications, such as sporty, decorative, paving, roof garden, and public landscape [1]. These textiles are subjected to different kinds of forces and deformations. One of the important deformations is compression and recovery after the load removal. It has been shown that the loss of thickness in artificial grass is highly affected by their compression behavior.

In recent years, many researchers have taken interest in the experimental study of the compression of textile product under dynamic loading. Sengupta *et al.* [2] found that once the ratio of the reinforcing material weight to the layer weight is decreased, the loss of thickness is reduced in dynamic loading. Kothari and Das [3] investigated the effect of dynamic loading on the compression properties of three types of fabrics: polyester needle-punched spun-bond, polypropylene needle-punched surface calendared spun-bond, and polypropylene thermally bonded spun-bond fabrics. They observed that polyester needle-punched spun-bond fabrics underwent the highest reduction in thickness. It is followed by needle-punched surface calendared spun-bond and thermally bonded spun-bond fabrics. A rheological model consists of mechanical elements to explain the behavior of nonwoven fabrics under compression load is developed by Krucinska *et al.* [4]. The effect of dynamic loading on jute and jute-polypropylene blended needle-punched nonwoven fabrics was investigated by Sengupta *et al.* [5]. As they observed, with an increase in the cycles of dynamic loading, the loss of thickness increased too. It was also found that the loss of thickness decreases with an increase in punch density, depth of needle penetration, and area density too. Debnath and Madhusoothanan [6] studied the effects of fabric weight, fiber cross-sectional shapes, and reinforcing materials on the compression properties of polyester needle-punched nonwoven fabrics including initial thickness, the rates of compression, thickness loss, and compression resilience. Their results showed that the initial thickness, compression, and thickness loss are higher in fabrics with no reinforcing materials. Das *et al.* [7] investigated the effects of certain parameters on the compression properties

A.A. Azami and P. Payvandy
Textile Engineering Department, Yazd University, Yazd, Iran.

M.M. Jalili
Mechanical Engineering Department, Yazd University, Yazd, Iran.

Correspondence should be addressed to P. Payvandy
e-mail: peivandi@yazd.ac.ir

of needle-punched nonwoven fabrics. Those parameters included fabric mass per unit area, needling density and the proportion of shrinkable acrylic fibers in the blend. It was shown that needling density and mass per unit area have significant effects on the compression, recovery, and resilience of needle-punched nonwoven fabrics, but shrinkable acrylic proportion has no significant effect before steam treatment. However, after steam treatment, the proportions of shrinkable acrylic have significant effect on these parameters. Ceilk and Koc [8] investigated the thickness loss of Wilton-type carpets with different pile materials (e.g. wool, acrylic, and polypropylene) under dynamic loading. The statistical evaluations showed that pile materials and the number of impacts have significant effects on the mean thickness and thickness loss. For all the samples, it was observed that an increase in the number of impacts led to a decrease in mean thickness. Also, it was found acrylic carpets, compared to other carpets, are more capable of recovery after that dynamic loads are removed. Bariagi *et al.* [9] investigated the compression property of nonwoven fabrics under different pressures. They showed that compression and recovery percentages for 1 kPa to 9 kPa loads are higher than those for 1 kPa to 5 kPa loads for all samples. This is due to the higher compactness and packing fraction after the first-step loading. Vuruskan *et al.* [10] examined the influence of pile density and pile height on the thickness loss of carpets which were exposed to dynamic loading under different impacts. It was found that both pile density and pile height parameters have significant effects on the compression properties of carpets. A linear viscoelastic model for the recovery behavior of the machine-made carpet after a brief static loading was presented by Jafari and Ghane in 2016 [11]. Different combinations of spring and damper systems were considered to model the mechanical behavior of carpets. Their results showed that there was a reasonably good agreement between the Jeffrey's model and the experimental result. The results also revealed the linear standard model has poor regression for the recovery properties of cut pile carpets after static loading. Khavari and ghane in 2017 [12] used three different models to investigate the compression, decompression, and recovery of cut pile carpets under constant rate of compression. Maxwell mechanical model, linear and nonlinear three-element models were used to simulate the compression and recovery behavior of the carpet samples. Results showed that the three-element model consists of a Maxwell body paralleled with a non-linear spring could explain compression and decompression behavior more accurately than Maxwell and linear models. Jafari and Ghane in 2017 [13] studied the effect of UV radiation on the recovery behavior of pile carpet after static loading through analytical and viscoelastic modeling. They showed that the thickness loss and the maximum compression were both higher at longer UV exposure times. In subsequent work by Jafari and Ghane in 2018 [14], two different mechanical models including linear and nonlinear Jeffrey's model were used to investigate the recovery property of machine made carpet under heavy static loading. Their results showed that the nonlinear Jeffrey's model indicates less value of speed of recovery at zero time in comparison to the linear model. So far, various experimental studies have been conducted on the compression behavior of textile productions under dynamic loading. In this study, we use the analytical investigation for the first time to predict the compression behavior on artificial grass. Thus, the aim of this study is to present a mechanical model based on a mass-spring-dashpot and estimate its parameters using imperialist competitive algorithm to explain the compression properties of artificial grass under dynamic loading.

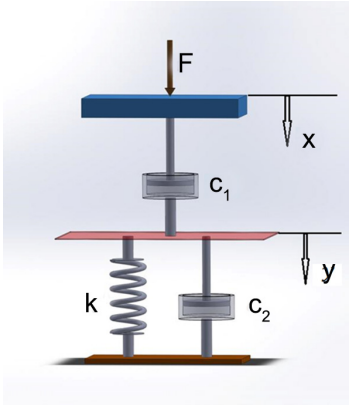

Fig. 1. Linear Jeffrey's model.

A. Mechanical Model

To investigate the compression behavior of artificial grass, a mechanical model known as Jeffrey's II model is used in this section. It consists of a Voigt-Kelvin unit that is placed in series with a linear dashpot. The schematic diagram of the model is presented in Fig. 1.

As the figure suggests, F is the compressive force applied to the model, k is the linear spring constant (N/m), and c_1 and c_2 are the dashpot constants (N.s/m).

In a Jeffrey's II model the forces in the dashpot c_1 and in the Voigt-kelvin element are the same. So, the compressive force is obtained using Eqs. (1) and (2) [15]; hence,

$$F = ky + c_2\dot{y} \tag{1}$$

$$F = c_1(\dot{x} - \dot{y}) \tag{2}$$

Where, x and y are the textile and Voigt-Kelvin unit

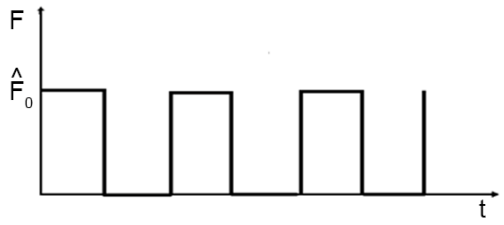

Fig. 2. Force F as a periodic impact force.

displacements, respectively.

As shown in Fig. 2, in dynamic loading, force F is a periodic impact force. Therefore, it can be expressed in the form of a Fourier series expansion with a set of harmonic forces in accordance with Eq. (3) [16]:

$$F(t)=\frac{f_0}{2}+\sum_{n=1}^{\infty}(f_n\cos\omega_n t+p_n\sin\omega_n t) \tag{3}$$

Where, F(t) is a periodic function with periodic interval T. Parameters f_n and p_n are obtained using Eqs. (4) and (5):

$$f_n=\frac{2}{T}\int_{-\frac{T}{2}}^{\frac{T}{2}}F(t)\cos\omega_n t dt \tag{4}$$

$$p_n=\frac{2}{T}\int_{-\frac{T}{2}}^{\frac{T}{2}}F(t)\sin\omega_n t dt \tag{5}$$

In which:

$$\omega_1=\frac{2\pi}{T} \tag{6}$$

$$\omega_n=n\omega_1 \tag{7}$$

Also, Eq. (8) can be obtained by the substitution of Eqs. (4) and (5) in Eq. (3) as follows:

$$F=\frac{\hat{F}_0 t_0}{T}+\sum_{n=1}^{\infty}\frac{\hat{F}_0}{n\pi}\left(\sin\frac{2\pi n}{T}t_0\cos\omega_n t+\left(1-\cos\frac{2\pi n}{T}t_0\right)\sin\omega_n t\right) \tag{8}$$

B. Compression

According to Eq. (8), force F consists of three parts including the constant force ($\hat{F}_0 t_0/T$), cosine terms ($\hat{F}_0/n\pi$).sin($2\pi n/T$).t_0.cos$\omega_n t$ and sinusoidal terms ($\hat{F}_0/n\pi$) (1-cos $2\pi n/T$).t_0).sin$\omega_n t$. Since the model is linear, the superposition principle is applied to it. So, the response for each part is obtained individually. The response of the system to periodic loads can be obtained by the sum of the responses of individual parts.

C. Compression in Terms of Constant Force

By substituting of the constant force ($\hat{F}_0 t_0$)/T in Eqs. (1) and (2), the following expressions can be achieved:

$$F_{01}=\frac{\hat{F}_0 t_0}{T}=ky+c_2\dot{y} \tag{9}$$

$$F_{01}=\frac{\hat{F}_0 t_0}{T}=c_1(\dot{x}-\dot{y}) \tag{10}$$

As Eqs. (9) and (10) are solved, the textile displacement (x) is determined as follows:

$$x=\frac{F_{01}}{c_1}t+Be^{\frac{-k}{c_2}t}+\frac{F_{01}}{k}-\frac{A}{c_1} \tag{11}$$

D. Compression in Terms of Cos$\omega_n t$

Once the cosine terms are substituted in Eqs. (1) and (2), the following expressions are achieved:

$$F_{02}\cos\omega_n t=ky+c_2\dot{y} \tag{12}$$

$$F_{02}\cos\omega_n t=c_1(\dot{x}-\dot{y}) \tag{13}$$

$$F_{02}=\frac{\hat{F}_0}{n\pi}\sin\frac{2\pi n}{T}t_0 \tag{14}$$

The textile displacement for this case can be obtained by solving Eqs. (12) and (13) as follows:

$$x=F_{02}\left(\frac{1}{c_1\omega_n}+\frac{c_2\omega_n}{(c_2\omega_n)^2+k^2}\right)\sin\omega_n t+\frac{F_{02}k}{k_2+(c_2\omega)^2}\cos\omega_n t+Be^{\frac{-k}{c_2}t}-\frac{A}{c_1} \tag{15}$$

E. Compression in Terms of Sin$\omega_n t$

By the substitution of the sinusoidal terms in Eqs. (1) and (2), the following expressions can be achieved:

$$F_{03}\sin\omega_n t=ky+c_2\dot{y} \tag{16}$$

$$F_{03}\sin\omega_n t=c_1(\dot{x}-\dot{y}) \tag{17}$$

In which:

$$F_{03}=\frac{\hat{F}_0}{n\pi}\left(1-\cos\frac{2\pi n}{T}t_0\right) \tag{18}$$

If parameter 'y' is calculated from Eq. (16) and the response to Eq. (17) is substituted, the displacement of the textile can be derived as follows:

$$x=-F_{03}\left(\frac{1}{c_1\omega_n}+\frac{c_2\omega_n}{k^2+(c_2\omega_n)^2}\right)\cos\omega_n t-\frac{F_{03}k}{k^2+(c_2\omega_n)^2}\sin\omega_n t+Be^{\frac{-k}{c_2}t}-\frac{A}{c_1} \tag{19}$$

The responses of Eqs. (1) and (2) to periodic excitation (3) can be obtained by the superposition of responses (11), (15), and (19) as follows:

$$x=\frac{\hat{F}_0 t_0}{2T}\left(\frac{1}{\kappa}+\frac{t}{c_1}\right)+Be^{\frac{-k}{c_2}t}-\frac{A}{c_1}+\sum_{n=1}^{\infty}\frac{\hat{F}_0}{n\pi}\sin\frac{2\pi n}{T}t_0$$
$$\left(\left(\frac{1}{c_1\omega_n}+\frac{c_2\omega_n}{(c_2\omega_n)^2+k^2}\right)\sin\omega_n t+\frac{k}{k^2+(c_2\omega_n)^2}\cos\omega_n t\right)+$$
$$\frac{\hat{F}_0}{n\pi}\left(1-\cos\frac{2\pi n}{T}t_0\right)\left(\left(-\frac{1}{c_1\omega_n}-\frac{c_2\omega_n}{k^2+(c_2\omega_n)^2}\right)\cos\omega_n t-\right.$$
$$\left.\frac{k}{k^2+(c_2\omega_n)^2}\sin\omega_n t\right) \quad (20)$$

Where, constants A and B can be determined using the initial conditions, i.e. x(t=0)=0 and $\dot{x}$(t=0)=0.

F. Estimation of the Excitation Force Amplitude

The maximum compression of the textile occurs when the velocity of the weight-piece becomes zero. In this state, dashpot force becomes zero. It can be ignored from the Jeffrey's II model. Therefore to estimate the parameter $\hat{F}_0$, the model was simplified as a mass and a linear spring according to Fig. 3.

The principle for the energy conservation of the system between the mass releasing time and the end time of impacts can be written as follows:

Parameter x can be calculated through solving Eq. (21) as follows:

$$mgh=-mgx+\frac{1}{2}kx^2 \quad (21)$$

The impact force is calculated by:

$$x=\frac{mg+\sqrt{(mg)^2+2kmgh}}{k} \quad (22)$$

$$\hat{F}=kx=mg+\sqrt{(mg)+2kmgh} \quad (23)$$

The technical data used for the estimation of the amplitude of the excitation force are presented in Table I.

II. EXPERIMENTAL

A. Materials and Methods

In this study, artificial grass from Zarifmosavar *et al.* [17] with average specification presented in Table II was used for samples.

TABLE I
TECHNICAL DATA USED FOR ESTIMATION OF $\hat{F}_0$

Parameter	Value
m (g)	1279
g (m/s^2)	9.8
k (N/m)	3.9×10^5
h (mm)	63

TABLE II
SPECIFICATIONS OF ARTIFICIAL GRASS SAMPLE

Specification	Value
Warp density (dm)	13
Weft density (dm)	18
Initial height of pile (mm)	12.15
Pile materials	PP 6-thereds+PE 2-theards
Pile count (dtex)	2200 PP+PE
Yarn profile	PE, monofilament+PP, curly fiber
Fibers color	Green+Lemon yellow

The initial thickness of the sample under a static pressure of (2±0.2) kPa was measured using a digital thickness tester made by Reessanj [18], as shown in Fig. 4. The measurement was based on the standard ISO 1765 [19]. The tester had an accuracy of 0.01 mm. According to the standard method, the sample was cut into 0.1×0.1 m^2 pieces. Five samples were prepared for each test and the mean value of the measurements was recorded. All the experiments were performed under the standard conditions of 20±2 °C and 65±2 RH% [20].

Fig. 5 shows a schematic of the compression value of the artificial grass under dynamic loading. As shown, x_0 is the initial thickness, x_1 refers to the thickness of the artificial grass after the compressive force applied to sample surface. The displacement is defined as (x_0-x_1). An increase in the number of impacts led to an increase in the displacement.

The thickness reduction of the artificial grass samples

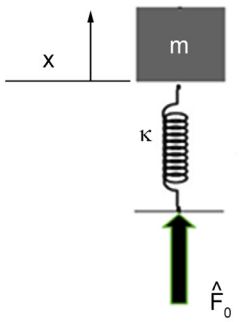

Fig. 3. Devised model to estimate the parameter $\hat{F}_0$.

Fig. 4. Determination of thickness device.

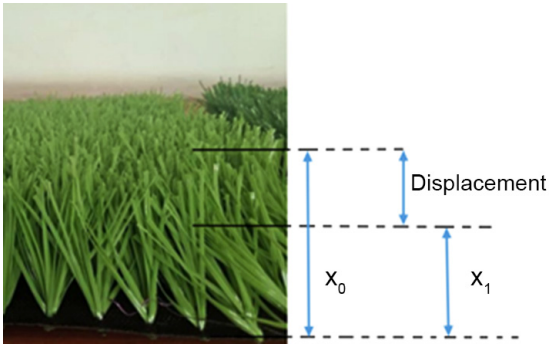

Fig. 5. Schematic diagram of thickness measurement.

was measured under dynamic loading. In order to measure the thickness reduction rate in dynamic loading, the samples were placed under dynamic loading in accordance with Standard ISO 2094 [21]. This standard specifies a method to determine the thickness loss of textile floor coverings under dynamic loading. According to ISO 2094, the weight-piece of a total mass (beater) 1279 g±13 g falls freely under gravity from a height of 63.5 mm±0.5 mm on to the specimen every 4.3 s±0.3 s. The thickness

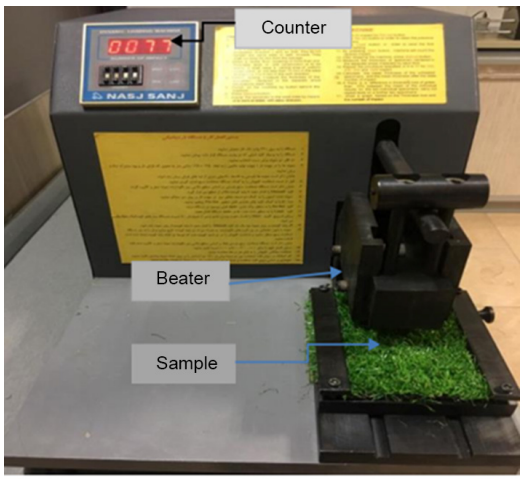

Fig. 6. A dynamic loading device.

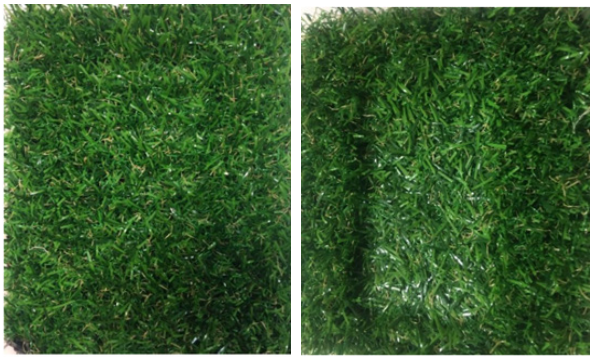

(a) (b)

Fig. 7. Images of sample: (a) before loading and (b) after loading.

measurements are made at intervals of up to 1000 impacts. A laboratory dynamic loading device made by Nasj Sanj from Iran was used to simulate the application of the dynamic loading, as shown in Fig. 6.

The samples were placed between two jaws and subjected to 50 impacts. Then the sample thickness in the two places was measured immediately. The loss of thickness in the samples under 50, 100, 200, 300, 500, 700, and 1000 impacts was also measured.

The images of sample before and after the test are presented in Fig. 7.

B. Imperialist Competitive Algorithm (ICA)

The imperialist competition algorithm (ICA) is an evolutionary computational method that finds the optimal answer to various optimization problems. This method provides an algorithm for solving mathematical problems by modeling [22]. In terms of application, the algorithm is in the category of evolutionary optimization algorithms such as genetic algorithms, particle swarm optimization, ant colony optimization, annealed simulation algorithm placed. Like all the algorithms in this category, the imperial competition algorithm forms the initial set of possible solutions. These early solutions are also known in the

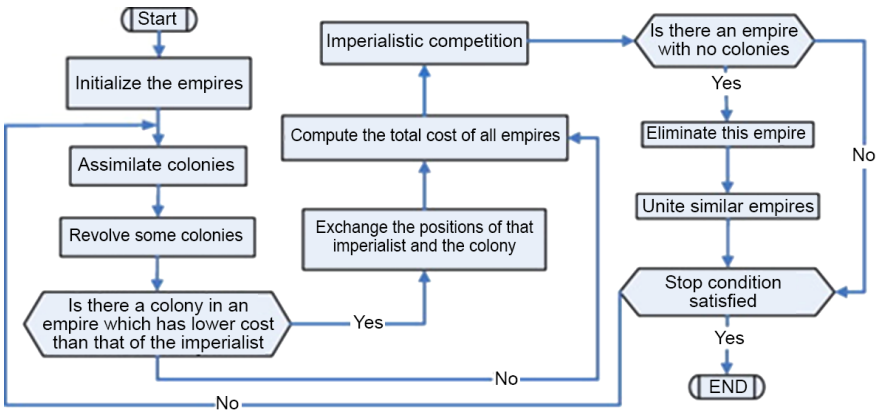

Fig. 8. Basic foundations of this algorithm are assimilation, imperialistic competition, and revolution [23].

TABLE III
ICA PARAMETERS

	Control parameters	Level		
		1	2	3
A	Number of generation	20	40	60
B	Assimilation coefficient	0.7	1.5	2.2
C	Number of imperials	10	30	50
D	Colonies share coefficient	0.7	1.5	2.2
E	Number of countries	100	300	500
F	Revelation rate	0.15	0.3	0.5

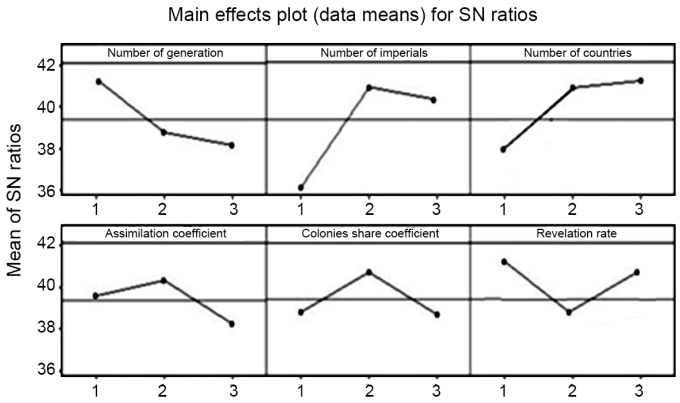

Fig. 9. Mean S/N ratio plot for each level of ICA factors.

genetic algorithm as "chromosome", in the particle swarm algorithm as "particle", and in the imperial competition algorithm as "country". The imperial competition algorithm with the specific process gradually improves these initial solutions (countries) and ultimately provides the appropriate solution to the optimization problem.

The flowchart of the imperialist competitive algorithm is shown in Fig. 8.

C. ICA Parameter Tuning

The important stage in the design of the experiment is the selection of the control factor. Table III represents ICA parameters used for initializing the optimization process. These parameters have been allowed to vary there different levels.

One of the important components of the imperialist competitive algorithm is the calibration of parameters which impress upon the performance of the algorithm. To define ICA parameter value and investigated how the mean and different parameter affect the model performance proposed, the Taguchi design of experiment is utilized.

D. Taguchi Method

The Taguchi method is a well-known technique that provides a systematic and efficient methodology for process optimization and is a powerful tool for the design of high quality systems [24]. It is commonly used in improving industrial product quality due to the proven success [25]. With the Taguchi method, it is possible to significantly reduce the number of experiment. The Taguchi method is not only an experimental design technique, but also a beneficial technique for high-quality system design. This technique helps to study the effect of many factors (variables) on the desired quality characteristics most economically. By studying the effect of individual factors on the results, the best factor combination can be determined.

By referring to the Taguchi standard arrays table, orthogonal arrays L_{27} , as the most suitable design, is used to tune the ICA parameters. Optimization was performed by MATLAB 2014. Fig. 9 shows the S/N ratio plot for each level of the factors of ICA after the experimental design for the problem mentioned. The results obtained by the Taguchi method indicated that A(3), B(3), C(1), D(1), E(1), and F(2) are the best combination of parameter for ICA.

III. RESULTS AND DISCUSSION

It should be mentioned that five samples were tested and the results were recorded based on the displacement value and standard deviation (SD) of the measurements, as illustrated in Table IV.

In this study, the compression behavior of artificial grass under dynamic loading was investigated. Eq. (20) was

TABLE IV
DISPLACEMENT OF THE ARTIFICIAL GRASS SAMPLES UNDER DYNAMIC LOADING

Impact (No.)	Time (s)	Displacement (mm)	SD
0	0	0.00	0.00
50	215	2.96	0.21
100	430	4.7	0.25
200	860	5.72	0.26
300	1290	6.3	0.33
500	2150	6.8	0.28
700	3010	7.02	0.24
1000	4300	7.00	0.21

TABLE V
LINEAR JEFFREY'S II MODEL PARAMETERS

Model	c_1 (N.s/m)	c_2 (N.s/m)	k (N/m)	A (m/s)	B (m)
Linear Jeffrey's II model under dynamic loading	4.39×10^{8}	4×10^{5}	3.9×10^{3}	2.7×10^{7}	6.8×10^{-3}

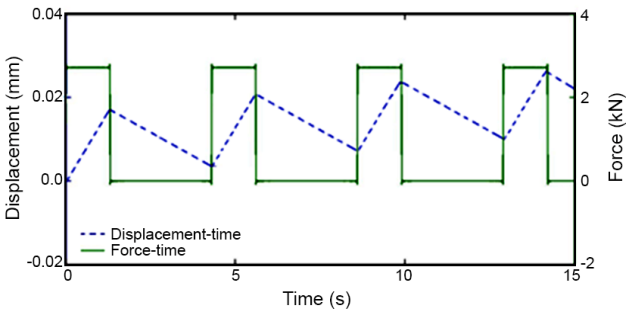

Fig. 10. Force and displacement versus time on a larger scale under four impacts (n=1000).

then adapted to the experimental data by using imperialist competitive algorithm. Determination of the best answer allowed the extraction of the linear Jeffrey's II models

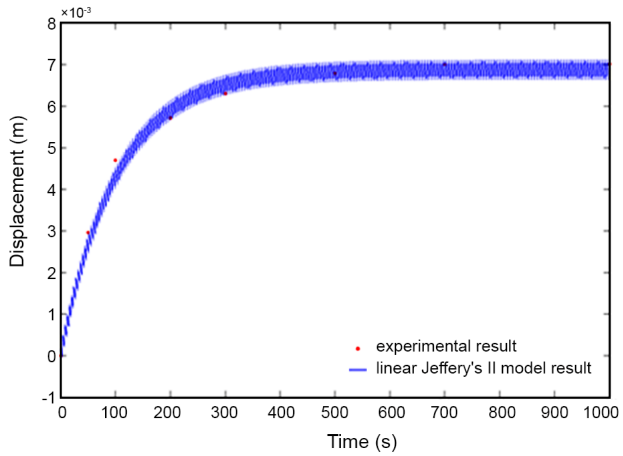

Fig. 11. Compression behavior of the samples.

TABLE VI
MEAN ABSOLUTE ERROR FOR THE LINEAR JEFFREY'S II MODEL UNDER DYNAMIC LOADING

Model	Loading	Compression error value (%)	R^2 (compression)
Linear	Dynamic	5.68	0.975

parameters. The parameters are presented in Table V.

Fig. 10 shows the changes of force and displacement versus time on a larger scale under four impacts.

Fig. 11 shows the experimental data and the results obtained from the linear Jeffrey's II model for the compression behavior (Eq. (20)) of the artificial grass samples after the exertion of 1000 impacts under dynamic

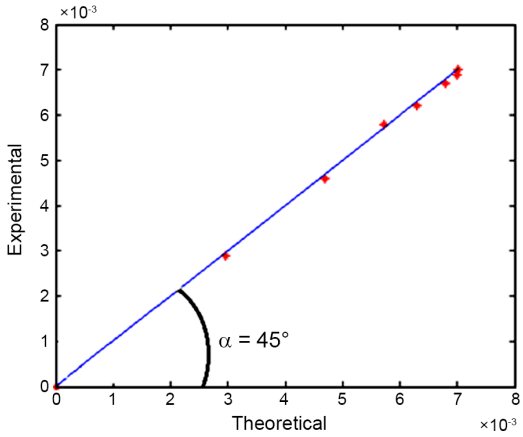

Fig. 12. Comparison of the experimental data and the results obtained from the linear Jeffrey's II model.

loading.

The mean absolute error and R^2 for compression behavior under dynamic loading in the linear model are presented in Table VI.

The results show that the rate of average error in the linear Jeffrey's II model under dynamic loading is 5.68% for compression behavior.

In order to determine predictive capability of the obtained model, the regression coefficient (R^2) was obtained. As emphasized before, the R^2 value is 97.5% for compression behavior. Comparison of the result presented in Fig. 12 shows good agreement between the experimental results and the results obtained from the presented model.

IV. CONCLUSION

In this study, the linear Jeffrey's II model was used as a mechanical model to predict the compression behavior of artificial grass under dynamic loading. The Fourier transform was also used to transform the periodic dynamic loading to the sum of the harmonic excitations. The loss of thickness for specific impact numbers was measured for the studied samples. The measurements were made for each sample under 50, 100, 200, 300, 500, 700, and 1000 impacts. Through solving the governing equations of the model, the system parameters were estimated by using imperialist competitive algorithm. The regression coefficient (R^2) for the theoretical and experimental diagram was obtained to predict the compression behavior of artificial grass under dynamic loading. The obtained values indicate that Jeffrey's II model is capable enough to predict the compression behavior of artificial grass under dynamic loading.

ABBREVIATIONS

A, B	Constants of the fabric displacement
c_1, c_2	Dashpot constants
CV	Coefficient of variation
F	Compressive force
f_n, p_n	Parameters of the Fourier series
$\hat{F}_0$	Amplitude of the excitation force
F_{01}	Constant force part of the Fourier series
F_{02}	Coefficient of terms of $\cos\omega_n t$ in the Fourier series
F_{03}	Coefficient of terms of $\sin\omega_n t$ in the Fourier series
g	Gravitational acceleration
h	Height of the weight-piece
k	Linear spring constant
m	Mass of the weight-piece
n	Number of impacts
R^2	Regression coefficient
T	Periodic interval of dynamic force
t_0	Initial time
x	Textile displacement
y	Voigt-Kelvin unit displacement
$\dot{x}$, $\dot{y}$	Time derivation of x and y
ω_n	n^{th} frequency of the Fourier series

REFERENCES

[1] https://www.royalgrass.com (2003-2018).

[2] A.K. Sengupta, A.K. Sinha, and C.R. Debnath, "Needle-punched non-woven jute floor coverings part II-dynamic loading and abrasion resistance", *Indian J. Text. Res.*, vol. 10, pp. 141-146, 1985.

[3] V.K. Kothari and A. Das, "Effect of dynamic loading on compressional behavior of spun bonded nonwoven fabric", *Geotext. Geomembr.*, vol. 13, no. 1, pp. 55-64, 1994.

[4] I. Krucinska, I. Jalmuzna, and W. Zurek, "Modified rheological model for analysis of compression of nonwoven fabrics", *Text. Res. J.*, vol. 74, pp. 127-133, 2004.

[5] S. Sengupta, P. Ray, and P.K. Majumdar, "Effect of dynamic loading on jute-based needle-punched nonwoven fabrics", *Indian J. Fibre Text.*, vol. 30, pp. 389-395, 2005.

[6] S. Debnath and M. Madhusoothanan, "Compression properties of polyester needle punched fabric", *J. Eng. Fiber. Fabr.*, vol. 4, no. 4, pp. 14-19, 2009.

[7] A. Das, R. Alagirusamy, and B. Banerjee, "Study on needle-punched non-woven fabrics made from shrinkable and non-shrinkable acrylic blends. Part I: compressional behaviour", *J. Text. Inst.*, vol. 100, pp. 10-17, 2009.

[8] N. Celik and E. Koc, "Study on the thickness loss of wilton-type carpets under dynamic loading", *Fibres Text. East. Eur.*, vol. 18, pp. 54-59, 2010.

[9] S.R. Bairagi, A.K. Singha, and S.C. Ray, "Studies of dimensional parameters and properties of newly developed nonwoven floor mats", *Int. J. Eng. Sci. Res. Tech.*, vol. 6, pp. 224-230, 2017.

[10] D. Vuruskan, E. Sarıoglu, H.I. Celik, and H.K. Kaynak, "Compression properties of woven carpet performance under dynamic loading", *Period. Eng. Nat. Sci.*, vol. 5, pp. 181-186, 2017.

[11] S. Jafari and M. Ghane, "An analytical approach for the recovery behavior of cut pile carpet after static loading by mechanical models", *Fiber Polym.*, vol. 17, no. 4, pp. 651-655, 2016.

[12] S. Khavari and M. Ghane, "An analytical approach for the compression and recovery behavior of cut pile carpets under constant rate of compression by mechanical models", *Fiber Polym.*, vol. 18, no. 1, pp. 190-195, 2017.

[13] S. Jafari and M. Ghane, "Analysis of the effect of UV radiation on the recovery properties of pile carpet after static loading through analytical and viscoelastic modeling", *J. Text. Inst.*, vol. 108, pp. 1905-1909, 2017.

[14] S. Jafari and M. Ghane, "Viscoelastic modeling of the recovery behavior of cut pile carpet after static loading: a comparison between linear and nonlinear models", *J. Text. Polym.*, vol. 6, no. 1, pp. 9-14, 2018.

[15] D.D. Joseph, *Fluid Dynamics of Viscoelastic Liquids*,1st ed., 1990.

[16] E. Keryszig, H. Kreyszig, and E.J. Norminton, *Advanced Engineering Mathematics*, 8thEd, John Wiley and Sons, 2014.

[17] Zarif Mosavar Holding, https://www.zarifmosavar.com (1984, accessed 21 October 2005).

[18] Reessanj knowledge Economy Company, https://www.reessanj.ir.

[19] ISO 1765, Machine Made Textile Floor Coverings-Determination of thickness, 1986.

[20] ISO 139, Textiles-Standard Atmospheres for Conditioning and Testing, 2005.

[21] ISO 2094, Textile Floor Coverings-Determination of Thickness Loss Under Dynamic Loading, 1999.

[22] M. Kargar and P. Payvandy, "Optimization of fabric layout by using imperialist competitive algorithm", *J. Text. Polym.*, vol. 3, no. 2, pp. 55-63, 2015.

[23] P. Payvandy and S. Ebrahimi, "Optimization of the thread take-up lever mechanism in lockstitch sewing machine using the imperialistic competitive algorithm", *J. Text. Polym.*, vol. 3, no. 1, pp. 12-19, 2015.

[24] G. Taguchi, S. Chowdhury, and Y. Wu, "*Taught Quality Engineering Handbook*", Wiley New Jersey, 2005.

[25] V. Mozafary and P. Payvandy, "Definition of mass spring parameters for knitted fabric simulation using the imperialist competitive algorithm", *Fibres Text. East. Eur.*, vol. 1, no. 25, pp. 66-74, 2017.